Journal of King Saud University – Science 33 (2021) 101453

Contents lists available at ScienceDirect

Journal of King Saud University – Science

journal homepage: www.sciencedirect.com

Original article

Hybrid optimization assisted deep convolutional neural network for hardening prediction in steel

Changhong Li [a,b], Chenbo Yin [a,*], Xingtian Xu [c]

[a] College of Mechanical and Power Engineering, Nanjing Tech University, Nanjing, Jiangsu 211816, PR China
[b] School of Metallurgical Engineering, Anhui University of Technology, Ma'anshan, Anhui 243002, PR China
[c] Nanjing Iron and Steel Co., Nanjing, Jiangsu 210035, PR China

ARTICLE INFO

Article history:
Received 21 December 2020
Revised 14 April 2021
Accepted 17 April 2021
Available online 21 May 2021

Keywords:
Hardening
Prediction
Steel
Mechanical
SL-DU model
Deep learning

ABSTRACT

Hardness is a property that prevents forced scraping or surface penetration of material surfaces against deformation. Indeed, some methods in the tradition of forecasting the mechanical properties of the steel used to recommend a new hardening forecast using a profound learning model. More particularly, an Optimized Deep Convolutional Neural Network (DCNN) framework is used that makes the prediction more accurate and precise. The input given to the model is the chemical composition of steel along with the distance from the quenched end, which directly predicts the hardening of steel as the model already knows of it. Moreover, to make the prediction more accurate, this paper aims to make a fine-tuning of Convolutional layers in DCNN. This paper suggests a new hybrid algorithm for optimal tuned, which is then hybridized Sea Lion Optimization (SLNO), Dragonfly Algorithm (DA), and Sea Lion insisted on Dragon Fly Modification (SL-DU). This is an optimal tuning. Finally, the performance of the proposed work is compared and validated over other state-of-the-art models for error measures. Finally, the performance of the adopted system was evaluated compared with other traditional systems and the results were achieved. According to the analysis, the MAE of the pattern used for distance 1.5 was 77.16%, 9.84%, 12.71%, and 23.36% better than regression, MVR, ANN, and CNN.
© 2021 Published by Elsevier B.V. on behalf of King Saud University. This is an open access article under the CC BY-NC-ND license (http://creativecommons.org/licenses/by-nc-nd/4.0/).

1. Introduction

The arithmetical evaluation of hardness distribution (Monnet et al., 2019a, 2019b; Oh and Ki, 2017) in quenched steel samples remains one of the best techniques for computing the steel quenching phenomenon and it also aids in the prediction of mechanical characteristics of steel specimen. Toughness, fatigue, and strength characteristics of steel could be approximated depending on the hardness of steel (Razavi et al., 2016; Latchoumi et al., 2019). Prediction of fatigue, strength, hardness, and beginning of cracks in steel specimen can be carried out using computer simulation. Toughness, fatigue, and strength characteristics of tempered and quenched steel are directly dependent on the microstructure of steel (Domański and Bokota, 2015; Nath et al., 2019). For overcoming this criterion, two major issues have to be resolved while cooling the steel: predicting the temperature changes, and predicting the mechanical properties and microstructure composition. The mathematical model of steel cooling depends on the calculated interval of cooling from "800 to 500 °C" (Iob et al., 2015; Torabi and Kamyab, 2019; Ranjeeth et al., 2019).

Bending procedures are commonly used in many manufacturing segments to create a wide range of geometric forms, including complicated ones, from raw materials or components. Bending is the uniform deformation of materials, typically flat plates or metal strips. In the longitudinal direction of the sheet or strip, on a straight line that is in the neutral and natural plane. It is thus used to bend flat leaves into very simple shapes (e.g., V-shaped and U-shaped) into a basic mold. The most significant disadvantage of the flexion process is the phenomenon of elastic return, which, if not properly managed, can result in injury. It causes serious errors in the part's final form, endangering the process's efficiency. The energy accumulated within the machined workpiece during plastic deformation during the bending process induces the elastic return phenomenon. Curved materials' elasticity can be surpassed while

* Corresponding author.
E-mail address: yinchenboo@163.com (C. Yin).
Peer review under responsibility of King Saud University.

Production and hosting by Elsevier

https://doi.org/10.1016/j.jksus.2021.101453
1018-3647/© 2021 Published by Elsevier B.V. on behalf of King Saud University.
This is an open access article under the CC BY-NC-ND license (http://creativecommons.org/licenses/by-nc-nd/4.0/).

still maintaining a residual elasticity on the inside. The energy contained inside the material can be released when the stresses are extracted at the end of the bending phase (Bernd et al., 2016; Tani et al., 2008; Shamsaei and Fatemi, 2009; Yin et al., 2010; Monnet and Mai, 2019; Schönbauer et al., 2016; Srinivas et al., 2016).

The specimen points include certain hardness, which could be approximated by converting the results of cooling time to hardness (Latchoumi et al., 2019). The cooling time at the specimen point could be predicted using the finite volume technique, which offers the arithmetical cooling simulation. In the literature (Wang et al., 2013; Castin et al., 2011; Sorsa et al., 2012), GA and ANN approaches were deployed for predicting and optimizing numerous features of the components. The phenomenon related to heat management is multifaceted and not yet described adequately. Enhancement in the domain of arithmetical solutions is mainly forced by industries that are striving for cost minimization and those industries that are demanding improvements on steel treatment (Özel and Nadgir, 2002; Javaheri et al., 2019; Song and Choi, 2003; Loganathan et al., 2017).

In recent times, "laser transformation hardening" technology has attained a huge interest in enhancing the wear resistance, hardness, and strength of steel. Different from other hardening approaches, laser hardening was dependent on a localized and precise heat source, which produces much higher intensities that remains idyllic for excellent hardening and rapid cooling quality (Masadeh et al., 2019; Jafari and Chaleshtari, 2017; Ranjeeth et al., 2020; Ding et al., 2019). In laser hardening, the attainment of essential hardness is important when reducing the thermal deformation as it necessitates higher precision. However, fulfilling both deformation and hardness requirements is a demanding task, and an optimal predictive approach should be implemented for reducing the costs and time significantly and to discover the desired processing conditions.

Following is the main contribution of this paper

The presented framework establishes a novel hardening prediction of steel using an optimized DCNN framework, which makes the prediction more precise and accurate.

At first, the inputs used to train the model are certain chemical composition of steel along with the distance from the quenched end, by which the hardening of steel could be directly predicted while testing.

Also, to make the prediction more precise, the work is extended to make a fine-tuning of Convolutional layers in DCNN, for which the SL-DU is exploited.

The efficiency of the device implemented is eventually measured against other cutting-edge systems and the results are achieved.

The arrangement of the paper is given as Section II analyses the review. Section III portrays the materials and methods and section IV portrays the framework of the proposed harden ability prediction. Further, section V illustrates the optimal tuning of the Convolutional layer by the proposed hybrid algorithm. Section VI portrays the results and the paper is concluded by section VII.

1.1. Literature review

1.1.1. Related works

ASSs were analyzed to the fundamental mechanisms and microstructure characteristics of plastic deformation. Also, the constitutive equations were adopted in this work for evaluating the grain size effect, dislocation network, solute clusters, and dislocation loops, and so on. It was revealed that irradiation hardening was attained systematically without any adaptable constraints. Finally, the findings of the analysis have shown that the introduced plan is superior to other schemes as regards hardness prediction.

3-D thermal introduced to aided by a methodical investigational study, for which "multi-mode fibre laser" was deployed for developing predictive schemes for thermal deformation and hardness of AISI H13 tool steel (Razavi et al., 2016; Oh and Ki, 2019). Using the established approach, the "ECT and ECDT" were evaluated by recording the temperature. Also, the adopted scheme aided in predicting the behaviours of thermal deformation and hardness efficiently and it had also enhanced the efficiency of the system.

Introduced a new model, where the plastic behaviour of RPV steels was portrayed by constitutive formulations. The stress of flow was disintegrated into its basic elements related to the microstructure characteristics like dislocation network, carbides, and so on. In the end, the emission defects were taken into account for exploiting the dynamics and atomistic outcomes. Finally, the impact of the solute cluster was examined briefly for the strength and cluster size, and density.

ANN was exploited for modelling the correlation among temperatures and aging times to the respective hardness. Moreover, GA was deployed for finding the optimal temperature and aging time for attaining the maximal value of hardness. Here, in this work, the ANN approach was deployed as the fitness function in GA. At last, the adopted scheme was examined by carrying out experimentations using the predicted constraints.

The differential hardening model developed which was observed experimentally in numerous commercially accessible steel sheet elements. Also, "Crystal plasticity theory" was exploited for analyzing various single-phase steels, and also the impact of hardening was noted under varying loading conditions. In the end, analysis outcomes have demonstrated the enhancement of the suggested model in terms of accuracy and hardening.

A new approach discovered that portrayed the procedures of hardening the steel. Accordingly, the initial priorities were offered to the thermal phenomenon, mechanical phenomenon, and phase transformations. Here, arithmetical approaches for phase transformations and phase computations were formulated depending upon the continuous heating and cooling of steel. Also, better hardening efficiency was found to be offered by the suggested model when compared to the other schemes.

Kinematic hardening implemented which was exploited for predicting the ratcheting behaviour of CSMs. The presented approach concerned more with improving the ratcheting predictions for CSMs by exploiting a novel generalized technique Moreover; the constraints of the scheme were optimized using the GA scheme, which and predicted the ratcheting performance more precisely.

A novel plasticity approach developed that depending on Hill's criteria. The presented scheme had offered a 3D description of anisotropic performance that addressed the malleable hardening in entire directions. Furthermore, a Lode angle effect was also established that provided descriptions regarding the shear stress conditions. The presented approach was examined and regulated with a fine laboratory set up for attaining high-grade steel pipelines. Finally, the outcomes had demonstrated the superior performance of the suggested system, and more particularly, it revealed its capability in predicting the hardness.

1.1.2. Review

Table 1 shows the reviews on predicting the hardening behavior of steel. At first, the Self-consistent method was introduced, which maximizes the reliability and it also offers a higher prediction on yield stress. However, the Avalanche term has to be focused more. FEM was exploited in that offers fast cooling and also provides improved accuracy, but it has to focus more on hardness analysis. FEM model has been used that offers a better estimation of macro-

Table 1
Review on Traditional Hardening Prediction Behaviour of Steel.

Author [citation]	Adopted methodology	Features	Challenges
Monnet and Mai	Self-consistent method	• Offers prediction on yield stress • Improved reliability	• Avalanche term has to be considered.
Oh and Ki	FEM	• Fast cooling • Improved accuracy	• Have to focus more on hardness analysis.
Monnet *et al.*	FEM model	• Better estimation of macroscopic response. • Optimal flow stress	• Needs analysis on room temperature.
Ali *et al.*	ANN scheme	• Improved hardness • Better accuracy	• Needs more consideration on temperature.
Philip *et al.*	ODF	• Increased accuracy • High strength	• Increased dimension leads to an increased number of calls.
Tomasz and Adam	FEM technique	• Increased cooling rate • Improved strength.	• Transformation plasticity has to be concerned more.
Atri *et al.*	GA	• Better stress level • Weight minimization	• Need consideration on the stress–strain response
Iob *et al.*	Hill(48) criterion	• Optimal strain • Improved torque	• Necking behavior has to be concerned.

scopic response and it also offers optimal flow stress. However, it needs analysis on room temperature. Also, the ANN scheme was implemented in that offers improved hardness and provides better accuracy; anyhow, it needs more consideration on temperature. ODF was presented in that offers increased accuracy with high strength, but, increased dimension leads to an increased number of calls. Moreover, the FEM technique was implemented in that provides an increased cooling rate along with improved strength. Anyhow, transformation plasticity has to be concerned more. Also, the GA model was suggested in which offer better stress level and it could offer better weight minimization. However, it requires consideration on stress–strain response. Hill (48) criterion was introduced in which provides optimal strain and also offers improved torque. However, necking behavior has to be concerned.

2. Materials and methods

2.1. Jominy test

"The Jominy end-quench test is the measure of the hardenability of steel, which is a measure of the capacity of the steel to harden in depth under a given set of conditions". The heat handling can also be selected carefully for minimizing thermal stresses and disturbances when manufacturing components of different sizes. The hardness capacity of stones is important to choose the right combination of alloy steel. Hardness is dependent on the chemical steel mix, which has also been influenced, for example, the astonishing temperature, by prior manufacturing conditions. Not only is it important to be aware of the specific information obtained from the test, but also how the information obtained from the Jominy test is used to know the impacts of alloys on steels.

The diagrammatic representation and dimensions of the Jominy test are revealed in Fig. 1. A steel cylinder with a length of 100 mm and diameter of 25 mm is subjected to heating for a predetermined

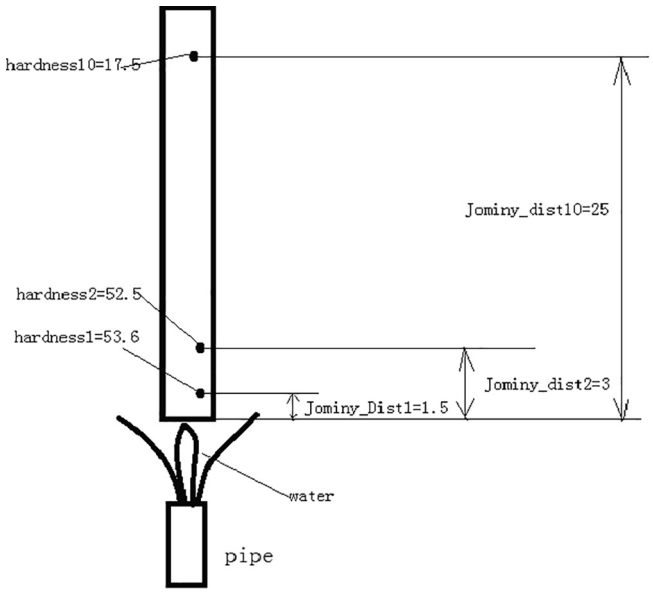

Fig. 1. Diagrammatic Representation of Jominy test Considered.

time within the austenitic area and it is quenched from its lower end with a standardized and controlled jet of water. The heat of water should lie between 15 and 25 °C. Based on the distance, the rate of cooling differs from 225 °C/s to 2 °C/s from the quenched end. Following the cooling process, the Jominy bar is refined in parallel to the axis of the cylinder on two sides. The outer region is grounded back for eliminating the issues related to decarburization and the hardening is evaluated from the quenched end at a certain period at this grounded surface. Thus, hardening could be measured at the cylinder axis in terms of distance from the quenched end. Fig. 2 shows the standard plot for depicting the hardenability of steel for varied distances from the quenched end.

For the proposed framework, the input data mentioned are the chemical composition of steels such as "Carbon (C), Manganese (Mn), Silicon (Si), Phosphorus (P), Sulphur (S), Copper (Cu), Nickel (Ni), Chromium (Cr), Vanadium (V), Titanium (Ti), Niobium (Nb), Molybdenum (Mo), Aluminium (Al), Calcium (Ca), Lead (Pb), Tin (Sn), Antimony (Sb), Boron (B), Bismuth (Bi)". Along with this, the distance from the quenched extremity is also considered. The formula of the respective chemical composition of the element is given in Table 2.

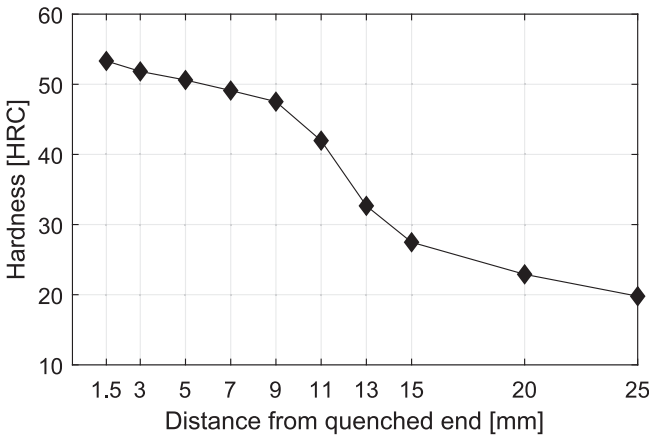

Fig. 2. Hardenability of Jominy test.

Table 2
Formula for chemical composition of steel.

Elements	Formula
ceq1	C + Mn/6
ceq2	C + Mn/6+(Cr + V + Mo)/5+(Cu + Ni)/15
ceq3	C + Mn/6 + Si/24 + Ni/40 + Cr/5 + Mo/4 + V/14
ceq4	C + Mn/6 + Cu/24 + Ni/20+(Cr-V)/10-Mo/50
ceq5	C + Si/30+(Mn + Cu + Cr)/20 + Ni/60 + Mo/15 + V/10 + B*5
ceq6	C + Mn/6 + Si/24 + V/14
ceq7	C + Mn/6+(Cr + V + Mo)/5
ceq8	C + Mn/6+(Cr + Mo + V)/5+(Ni + Cu)/15 + B*15
Pcm	C + Si/30+(Mn + Cu + Cr)/20 + Ni/60 + Mo/15 + V/10 + B*5
Psr	Cr + Cu + 2*Mo + 10*V + 7*Nb + 5*Ti-2
T_E	1536.6-(88*C + 8*Si + 5*Mn + 30*P + 25*S)
ceq9	C + Si/6 + Mn/4.5 + Ni/15 + Cr/4 + Mo/4.5 + 1.8*V
T_C < 0.5	1536.6-(88*C + 8*Si + 5*Mn + 5*Cu + 1.5*Cr + 4*Ni + 2*Mo + 18*Ti)
T_C > 0.5	1530.6-(76*C + 8*Si + 5*Mn + 1.5*Cr + 4*Ni + 2*Mo + 18*Ti + 5*Cu) + 5
NICRCU	Ni + Cr + Cu
VNBTI	V + Nb + Ti
Al/N	Al/N
NICRCUMO	Ni + Cr + Cu + Mo
ASPBSNSB	As + Pb + Sn + Sb
ASPBSNSBBI	As + Pb + Sn + Sb + Bi
ComY	(Si + Mn)*(P + Sn)*10
ComX	(10*P + 5*Sb + 4*Sn + As)/100
TI/N	Ti/N
Ca/S	Ca/S

2.2. Framework of proposed hardenability prediction

The architecture of the proposed hardenability prediction model of the steel is demonstrated by Fig. 3. In this work, the chemical composition of steels such as C, Mn, Si, P, S, Cu, Ni, Cr, V, Ti, Nb, Mo, Alt, Ca, Als, Pb, Sn, Sb, B, W, H, Zr, Co, Bi, Zn, Ta, Se and F along with the distance parameters is given as inputs to DCNN framework. More particularly, to make the prediction more accurate, this work aims to optimize the convolutional layers of DCNN using the SL-DU algorithm, which ensures accurate prediction results.

2.3. Deep convolutional neural networks

DCNNs [26] are CNNs that include numerous layers and it follows the hierarchical principle as given by Fig. 4. Following numerous Convolutional layers, deep CNNs usually include one or more wholly-connected layers, i.e., layers with denser weight matrix W. Apart from the input, spatial location is both quite inappropriate and partially lost and hence the local receptive regions of CNNs cannot be used. In case, if the classifier necessitates input quantity

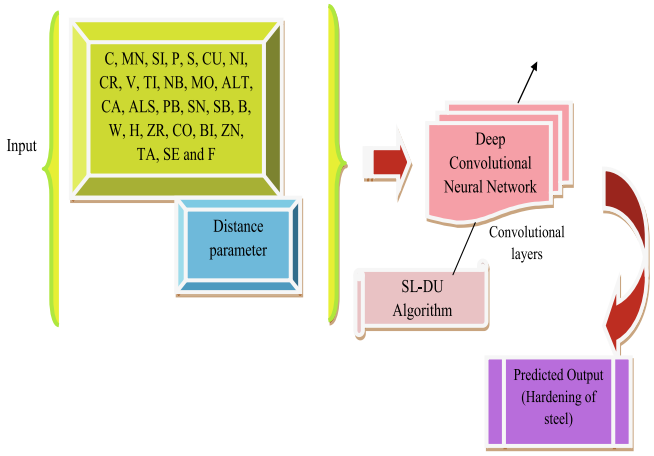

Fig. 3. Diagrammatic illustration of the proposed framework.

that behaves similarly to probabilities, the output phase can be a "softmax function" as given in Eq. (1), in which 1 denotes a column vector of ones.

$$u = \sigma(x) = \frac{\exp(x)}{1^T \exp(x)} \tag{1}$$

In practice, the entire quantities are made positive by exponential, and normalization guarantees that the entries of$u$ adds up to 1. In general, the "softmax function" could be observed as a multidimensional generalization of the sigmoid function exploited in logistic regression (LR). This function is so-called "softmax" as one of the $x_i$entries, e.g.x_{i0}, is higher over the others, then$1^T \exp(x) \approx \exp(x_{i_0})$ and hence Eq. (2) is formulated. The above function efficiently performs as an indicator among the highest entry in$x$. Thus Eq. (3) is formed.

$$u_{i_0} \approx 1 u_i \approx 0 i \neq i_0 \tag{2}$$

$$\lim_{\alpha \to \infty} x^T \sigma(\alpha x) = \max(x) \tag{3}$$

In short, DCNN carries out the below formulations mentioned in Eq. (4)-Eq. (7), in which the output activation function $f_x$might be "softmax", identity, or other function.

$$z^{(0)} = z \tag{4}$$

$$z^{(q)} = \pi\left(f\left(W^{(q)} \tilde{z}^{(q-1)}\right)\right) \quad for \;\; q = 1, \ldots, Q_c \tag{5}$$

$$z^{(q)} = f\left(W^{(q)} \tilde{z}^{(q-1)}\right) \quad for \;\; q = Q_c + 1, \ldots, Q \tag{6}$$

$$x = f_x\left(z^{(Q)}\right) \tag{7}$$

The matrix$W^{(q)}$ includes $F^{(q)}$rows and $F^{(q-1)} + 1$columns with $F^{(0)} = F$and $F^{(q)}$for$q > 0$, which is equivalent to the output count in $q^{th}$the layer. The initial $Q_c$layers are convolution and the remaining ones are wholly connected.

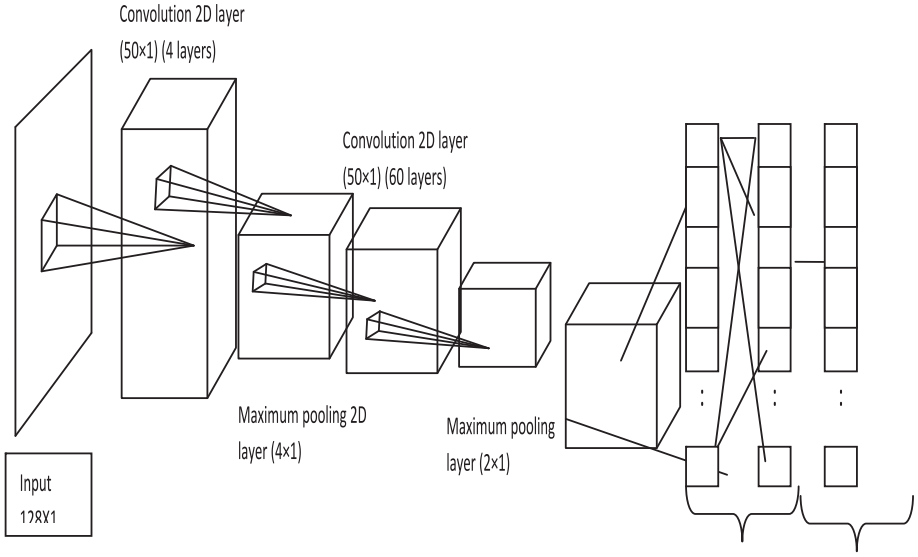

Fig. 4. Pictorial demonstration of DCNN framework.

3. Optimal tuning of Convolutional layer by Proposed hybrid Algorithm

3.1. Solution encoding and objective function

In the presented work, for better harden ability prediction of steel, it is planned to tune the optimal Convolutional layers (Q_c)of DCNN. The solution encoding for the proposed prediction model is shown in Fig. 5, which $N_b$represents the count of Convolutional layers in DCNN. Here, the objective function *(OF)* of the presented work is defined in Eq. (8), where*Err* denotes the error between actual and predicted value.

$$OF = Min(Err) \tag{8}$$

3.2. Conventional dragonfly algorithm

The core inspiration of the DA model [25] is the swarming processes associated with the two main steps:(i) Exploration and (ii) Exploitation. Both phases are modeled as follows: as in Eq, the separation formula is evaluated. An error occurred (9), which $S_l$reveals thel^{th}, S indicates the location of the neighboring person, and N indicates the count of the people around him.

$$C_i = -\sum_{l=1}^{M} S - S_l \tag{9}$$

Alignment is measured as defined in Eq. (10), which $Q_l$signifies the velocity of the l^{th}neighboring individual. Also, the formulation for cohesion is given by Eq. (11), whichS_l specifies, the position of thel^{th} neighboring individualN_b symbolizes the neighbor count and$S$ signifies the position of the current individual. Attraction to a food resource is computed by Eq. (12), whichS^+ corresponds to the position of the food source and$S$ signifies the current individual position.

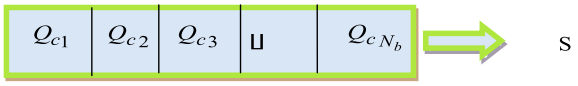

Fig. 5. Solution encoding.

$$B_i = \frac{\sum_{l=1}^{M_b} Q_l}{M_b} \tag{10}$$

$$O_i = \frac{\sum_{l=1}^{M_b} S_l}{M_b} - S \tag{11}$$

$$F_i = S^+ - S \tag{12}$$

Eq. (13) determines the distraction to an opponent, whichS^- describes the enemy's position and$S$ denotes the present position of individuals. To update and carry out movements of dragonflies in a space of discovery, the evaluation of two vectors is a phase (ΔS) and position (S).

$$E_i = S^- + S \tag{13}$$

The step vector exposes the moving direction of the dragonfly, as computed in Eq. (14). Here,C_i indicates the separation of i^{th}individual,q denotes the separation weight, $a$denotes the alignment weight,O signifies the i^{th}individual cohesion, c refers to cohesion weight, B andF_i points to alignment and food resource of i^{th}individual respectively$f$ symbolizes food factor, $b$corresponds to enemy factor, w refers to the inertia weight, E_i signifies enemy's position of the i^{th}individual and itindicates iteration counter.

$$\Delta S(it+1) = (qC_i + aB_i + cO_i + fF_i + bE_i) + w\Delta S(it) \tag{14}$$

The position vectors are manipulated by Eq. (15) after the evaluation of the phase vector, where the latest version is shown.

$$S(it+1) = S(it) + \Delta S(it+1) \tag{15}$$

It is important to travel around the discovery region where there are no neighboring solutions to boost the stochastic efficiency of the artificial floats. Under these conditions, the location of the dragonfly is updated by Eq. (16), in which the vector position dimension is represented and the current iteration is represented.

$$S(it+1) = S(it) + Levy(z) \times S(it) \tag{16}$$

The Levy flight is evaluated by Eq. (17), whichη is a constant factor and $r_1 r_2$is the random numbers that are lying among [0, 1]. Further, δ is computed using Eq. (18), in which$\Gamma(x) = (x-1)$. Algorithm 1 depicts the pseudo-code of the conventional DA model.

$$Levy(x) = 0.01 \times \frac{r_1 \times \delta}{|r_2|^{\frac{1}{\eta}}} \tag{17}$$

$$\delta = \left(\frac{\Gamma(1+\eta) \times \sin(\frac{\pi\eta}{2})}{\Gamma\frac{(1+\eta)}{2} \times \eta \times 2^{(\frac{\eta-1}{2})}} \right)^{\frac{1}{\beta}} \tag{18}$$

Algorithm 1: Conventional DA algorithm [25]
Initialization
While end condition is not attained
  Evaluate the objective value of entire fireflies
  Update enemy and food source
  Update w,q ,a , c,*f* and b
  Compute*C*B sssso, E and F as per Eq. (9–13)
  Update the neighboring radius
  If a dragonfly involves one neighbor dragonfly,
    Update velocity as per Eq. (14)
    Update position as per Eq. (15)
  else
    Update the position vector as per Eq. (16)
  end If
  Verify novel positions, depending on variable boundaries
end While

3.3. Conventional SLnO algorithm

SLnO [24] is a recent optimization approach that is developed based on the hunting behavior of sea lions. The major stages regarding the hunting behavior of sea lions are

- Tracing and chasing of prey by their whiskers.
- Pursuing and encircling the prey by calling the sea lions of their subgroups to join them.
- Attacking the prey.

3.3.1. Mathematical Modeling

The SLnO scheme is described mathematically with four phases known as tracking, social hierarchy, attacking, and encircling prey.

3.3.2. Detecting and tracking phase

The whiskers allow the marine lion to detect the current bear, and to detect the location of the whiskers in the opposite direction to the water wave. The pulse of whiskers, though is smaller when their direction is equally present. Sealion learns the location of the prey and demands that its subgroup be combined to locate and pursue the prey. This sea lion is considered the pioneer in the field of hunting, and the other participants enter modified positions against the target prey. The goal probe is closer to the optimum solution. This mechanism is arithmetically specified as per Eq. (19), in which the distance amongst the sea lion and target prey is denoted by $\overrightarrow{Dis}$, the vector position of target prey and sea lion is pointed out by $\overrightarrow{M}(t)$ and $\overrightarrow{S}(t)$, correspondingly, t denotes the current iteration and the arbitrary vector is given by $\overrightarrow{G}$.

$$\overrightarrow{Dis} = \left| 2\overrightarrow{G}.\overrightarrow{M}(t) - \overrightarrow{S}(t) \right| \tag{19}$$

At subsequent iteration, the sea lion moves to the target prey to get closer. The arithmetical model of this mechanism is given by Eq. (20), in which the next iteration is specified $(t+1)$ and $\overrightarrow{H}$ gets gradually decreased over the iterations from 2 to 0.

$$\overrightarrow{S}(t+1) = \overrightarrow{M}(t) - \overrightarrow{Dis}.\overrightarrow{H} \tag{20}$$

3.3.3. Vocalization phase

Sea lions can stay alive both on land and water. The sound of sea lions in water can move four times faster than in the air. Numerous vocalizations are used by the sea lions for communication when chasing or hunting the prey. Also, they can detect the sound both on and under the water. Therefore, when it discovers a prey, it calls on other members for encircling and attacking the prey, which is mathematically designed as in Eq. (21), (22), and (23), in which the speed of the leader's sound is denoted by $\overrightarrow{S_{leader}}$, the sound's speed in air and water is symbolized as $\overrightarrow{P_2}$ and $\overrightarrow{P_1}$.

$$\overrightarrow{S_{leader}} = \left| \left(\overrightarrow{P_1}(1 + \overrightarrow{P_2}) \right) / \overrightarrow{P_2} \right| \tag{21}$$

$$\overrightarrow{P_1} = \sin\theta \tag{22}$$

$$\overrightarrow{P_2} = \sin\varphi \tag{23}$$

3.3.4. Attacking phase

During the exploration phase, the hunting mechanism of sea lions is performed under two stages that are described below:

Dwindling encircling approach: This mechanism is based on $\overrightarrow{H}$ the value in Eq. (20). Mainly, $\overrightarrow{H}$ is gradually minimized via a course of iteration from 2 to 0. This reducing factor directs the sea lion to forward on and to encircle the prey.
Circle updating position: The bait ball of fishes are chased and attacked by sea lion beginning from edges, which is given as in Eq. (21), where the distance among the sea lion and target prey is represented by $\overrightarrow{M}(t) - \overrightarrow{S}(t)$, the absolute value is referred by || and the random number between − 1 to 1 is denoted by *l*.

$$\overrightarrow{S}(t+1) = \left| \overrightarrow{M}(t) - \overrightarrow{S}(t).\cos(2\pi l) \right| + \overrightarrow{M}(t) \tag{21}$$

3.3.5. Prey Searching

Based on the best investigator in the exploratory process, the location update of sea lions is done. The quest agent's location update during the scan stage is based on the sea lion picked randomly. I.e. the SLnO algorithm performs a global search and determines the global optimal solution when $\overrightarrow{H}$ is higher than 1. This is explained by Eqs. (22) and (23). The pseudo-code of the conventional SLnO scheme is highlighted in Algorithm 1.

$$\overrightarrow{Dis} = \left| 2\overrightarrow{B}.\overrightarrow{S_{rnd}}(t) - \overrightarrow{S}(t) \right| \tag{22}$$

$$\overrightarrow{S}(t+1) = \overrightarrow{S_{rnd}}(t) - \overrightarrow{Dis}.\overrightarrow{H} \tag{23}$$

3.4. Proposed Algorithm: SL-DU

For hardening prediction of the steel, this paper is designed to refine the Convolutionary layers of DCNN that can achieve a precise prediction. There is a suggestion for a new hybrid algorithm incorporating the ideas of DA and SLNO to resolve the limitations, such as poor convergence. In the traditional solution, DA is modified with levy according to Eq. The method of the hybrid algorithm is as follows: There was a mistake (16). In the proposed algorithm, the levy update of DA is evaluated by the position update of the SLnO algorithm. i.e. the levy update is as per Eq. (23) and the cor-

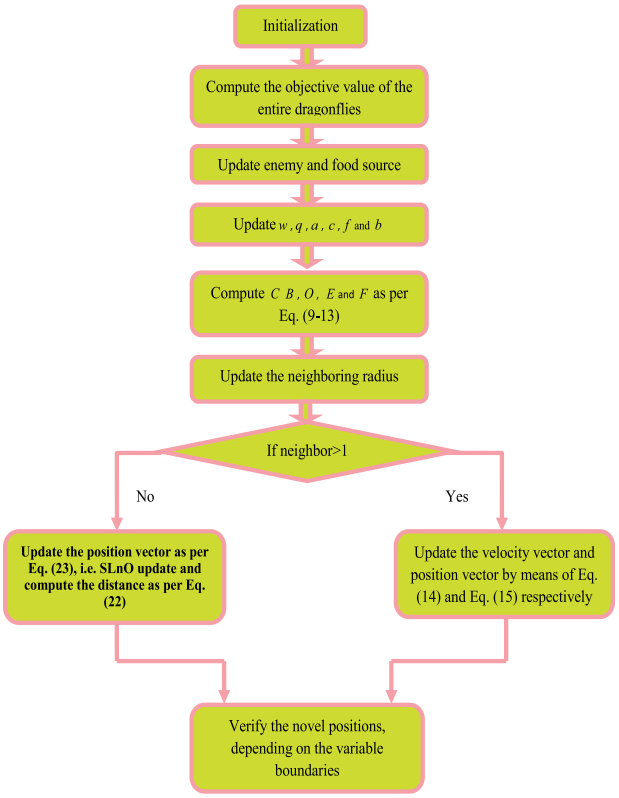

Fig. 6. Flowchart of proposed SL-DU model.

responding distance is computed using Eq. (22). The updated model is called the SL-DU model since it relies on a SLnO upgrade in DA. Algorithm 2 shows the pseudo-code of the SL-DU algorithm proposed. Fig. gives the representation of the flowchart (Fig. 6).

Algorithm 2: Proposed SL-DU model
Initialization
While the end condition is not attained
Evaluate the objective value of entire fireflies
Update enemy and food source
Update *w*,*q*,*a*, *c*,*f* and*b*
Compute*CBO*, *E*and *F* as per Eq. (9–13)
Update the neighboring radius
If a dragonfly involves one neighbor dragonfly,
Update velocity as per Eq. (14)
Update position as per Eq. (15)
else
Update the position vector as per Eq. (23), i.e. SLnO updateCompute the distance as per Eq. (22)
End If novel positions are checked, according to variable limit finish.

4. Results and discussions

4.1. Simulation procedure

The adopted hardening prediction of steel was executed in MATLAB using the SL-DU model and the corresponding outcomes were attained. The process of experimentation for data collection is mentioned in the above section. Here, the performance of the presented technique was compared over the other conventional schemes like regression [27], MVR [28], ANN [29], and CNN [30] to error measures like MAE, MAPE, RMSRE, and R-value. The R-value was computed as per Eq. (24).

$$R = 1 - abs\left[\frac{Sum[\text{Predicted} - \text{Target}]^2}{Sum[\text{Target}^2]}\right] \quad (24)$$

Further, To verify the work's results, statistical analytics was also performed. In the presented work, the analysis was carried out under two cases. Here, 321 records and 24 attributes were considered for experimentation (i.e. size of 321 × 24) and along with that, 10 values of distance (1.5, 3, 5, 7, 9, 11, 13, 15, 20, and 25) were also taken into account. Accordingly, each distance was added up with the attributes and thus, the size of the dataset turns out to be 321 × 25. Thus, **ten sets of data** were formed using ten values of distance. Under the first case, for all the ten sets of data, 70% was exploited for the training phase and the remaining 30% of data was exploited for the testing phase. Accordingly, the second case was carried out for five experimentations. During the 1st experimentation, the first two sets of data were exploited for the testing phase and the remaining eight sets of data were exploited for the training phase. Similarly, during the 2nd experimentation, the third set and fourth sets of data were exploited for the testing phase and the remaining datasets were exploited for the training phase. While carrying out 3rd experimentation, the fifth and sixth sets of data were exploited for the testing phase and the remaining datasets were exploited for the training phase. While performing the 4th experimentation, the seventh and eighth sets of data were exploited for the testing phase and the remaining datasets were exploited for the training phase, whereas, during 5th experimentation, the ninth and tenth sets of data were exploited for the testing phase and the remaining datasets were exploited for the training phase.

5. Result analysis under case 1

5.1. Analysis on Prediction

This section explains how much the mentioned methods correlate with the prediction accuracy. From the graphical representation (Fig S1 and S2), the x-axis declares the actual harden ability and the y-axis declares the predicted harden ability for varied distance values. Altogether, the graphs prove that the proposed method's predicted value is much closer to the actual value. However, conventional methods show their poor performance. In for an actual value of 0.94, the predicted harden ability output of the proposed is almost nearer to the actual value, whereas the values attained by the remaining methods scatter throughout the space. Similar results have been observed for all the distances. Thus the effectiveness of the proposed algorithm has been proved over other models.

5.2. Optimization Performance

The plots of the box are usually used to show details on the properties of the research conducted. Here, the analysis was carried out by plotting the fitness against varied iterations. Fig. S3 shows the optimization performance on the box plot for case 1. Since the goal or fitness function is to minimize errors, the plot needs to demonstrate that the proposed model progressively minimizes fitness. Fig S3 reveals the result for 25 iterations. As the iteration increases, the proposed model reveals gradual minimization of fitness. Thereby, at iteration 25, the least value is obtained that is in the range of 19 to 19.5.

5.3. Error Analysis

The error analysis of the proposed over traditional schemes is given by Table 3 on considering the overall values of distance. The error measures like MAE, MAPE, and RMSRE should be minimal for the adopted work, whereas the R-value should be higher to finalize precise prediction of the harden ability of steel. From Table 3, it is observed that the error value (MAE) obtained by the proposed model is linearly less than other models, which directly proves the betterment of the proposed model with precise prediction. Similarly, for MAPE, the least value 2.8297 is obtained by the proposed work, whereas the remaining models attain a higher value. The R-value evaluation is done as per Eq. (24), which should be higher when compared to other models. This is also proved by the proposed model with the utmost value of 0.99893.

Moreover, the analysis was held for the ten different distance values and the variation among the actual and predicted values during the testing phase are plotted in Tables S1–S4 concerning MAE, MAPE, RMSRE, and R-values respectively. From Tables S1–S4, the error measures are low for the presented method when evaluated over the traditional methods. Specifically, from Table S1, the MAE of the proposed scheme for distance 1.5 is 77.16%, 9.84%, 12.71%, and 23.36% better than the regression, MVR, ANN, and CNN. Also, from Table S2, the MAPE of the adopted scheme for distance 5 is 82.93%, 68.36%, 34.25%, and 9.64% superior to regression, MVR, ANN, and CNN models. From Table S3, the RMSRE of the suggested scheme is 90.29%, 42.65%, 57.1%, and 49.09% superior to regression, MVR, ANN, and CNN approach. Also, from Table S4, the R-value is higher for the adopted model, which is 21.75%, 2.87%, 0.63%, and 0.1% superior to regression, MVR, ANN, and CNN models Thus, the betterment of the adopted model is confirmed from the outcomes (Table S5 and S6).

5.4. Statistical Analysis

Since the *meta*-heuristic algorithms are intangible, the same outcome cannot be obtained. Thus, five times it is finished, and the best bad, middle, and standard deviation is defined. All the listed error measurements have been statistically evaluated. From the results, With decreased error behaviour, the presented plan achieved better performance than the other existing programs. More particularly, from Table S8, the mean of the proposed scheme for distance 1.5 is 77.16%, 9.84%, 12.71%, and 23.36% better than the regression, MVR, ANN, and CNN. Also, from Table S8, the standard deviation of the adopted scheme for distance 1.5 is 88.09%, 36.68%, 34.93%, and 8.49% better than the regression, MVR, ANN, and CNN models. Similarly, Table S9 summarizes the results under the median and worst-case scenario for varied distances. Thus, the predicting capability of the adopted scheme is proved to be efficient over the other traditional schemes.

5.5. Results analysis under case 2

Fig. S4 demonstrates the optimization performance on the box plot for case 2 by plotting the fitness against varied iterations. Here, the adopted work intends on error minimization and therefore, the plot should reveal a gradual minimization of fitness. The fitness is evaluated for 25 iterations and accordingly, a gradual minimization of fitness is attained by the presented model with an increase in the iteration.

5.5.1. Error Analysis

Fig. S5 shows the error analysis of the adopted model over traditional schemes by considering the overall values of distance. The analysis is carried out for error measures like MAE, MAPE, and RMSRE, which needs to be minimal for the presented scheme, while the R-value (computed as per Eq. (24)) should be high for accurate prediction of the hardenability of steel. Fig. S5(a) The SL-DU method followed for the prediction of hardening of steel for 5 sets of experiments shows the study of objective functions (error analysis). On the observation of the results obtained, the proposed solution in terms of different error measurements achieves increased efficiency over the other compared schemes. From Fig. S5(a), the adopted model in terms of MAE is 54.54%, 50%, 50%, and 50% better than the regression, MVR, ANN, and CNN schemes. From Fig. S5(b), the presented SL-FU model is 68%, 50%, 50%, and 50% better than the regression, MVR, ANN, and CNN schemes. On concerning the RMSRE from Fig. S5(c), the implemented scheme is 54.54%, 50%, 50%, and 50% better than the regression, MVR, ANN, and CNN approach. Also, from Fig. S5(d), the R-value of the adopted scheme is 11.11% better than the compared approaches. Thus, the enhanced performance of the proposed scheme is validated effectively.

6. Conclusion

The presented framework established a novel hardening prediction using an optimized DCNN framework, which makes the prediction more precise and accurate. At first, the chemical composition of steel along with the distance from the quenched end was given as input to the model, by which the hardening of steel could be directly predicted as the model already knows it. Also, to make the prediction more precise, this work intended to make a fine-tuning of Convolutional layers in DCNN, for which the SL-DU is exploited. Finally, the results of the implemented system were analyzed and achieved in comparison to other conventional schemes. The research, At last, the performance of the adopted scheme were evaluated over other traditional schemes and the outcomes were attained. From the analysis, the MAE of the adopted scheme for distance 1.5 was 77.16%, 9.84%, 12.71%, and 23.36% better than the regression, MVR, ANN, and CNN. Also, the MAPE of the adopted scheme for distance 5 was 82.93%, 68.36%, 34.25%, and 9.64% superior to regression, MVR, ANN, and CNN models. The RMSRE of the suggested scheme was 90.29%, 42.65%, 57.1%, and 49.09% superior to regression, MVR, ANN, and CNN approaches. The improvement of the scheme is thus seen.

The influence of the cryogenic treatment cycle on cooling speeds, retention temperature, and post-treatment income will be studied in the future to determine the best treatment cycle for maximum gain.

Table 3
Error analysis of the proposed over traditional schemes on considering overall distance values.

Methods	MAE	MAPE	RMSRE	R-value
Regression [27]	0.13271	20.732	0.2997	0.94356
MVR [28]	0.067547	10.316	0.12613	0.9893
ANN [29]	0.030937	4.7105	0.062807	0.99741
CNN [30]	0.042278	5.9307	0.072134	0.99531
SL-DU	0.019821	2.8297	0.035377	0.99893

Declaration of Competing Interest

The authors declare that they have no known competing financial interests or personal relationships that could have appeared to influence the work reported in this paper.

Appendix A. Supplementary data

Supplementary data to this article can be found online at https://doi.org/10.1016/j.jksus.2021.101453.

References

Castin, N., Malerba, L., Chaouadi, R., 2011. Prediction of radiation induced hardening of reactor pressure vessel steels using artificial neural networks. J. Nucl. Mater. 408 (1), 30–39.

Ding, S., Tian, G., Sutthaweekul, R., 2019. Non-destructive hardness prediction for 18CrNiMo7-6 steel based on feature selection and fusion of Magnetic Barkhausen Noise. NDT & E Int. 107, 102138. https://doi.org/10.1016/j.ndteint.2019.102138.

Domański, T., Bokota, A., 2015. The numerical model prediction of phase components and stresses distributions in hardened tool steel for cold work. Int. J. Mech. Sci. 96-97, 47–57.

Iob, F., Campanelli, F., Coppola, T., 2015. Modelling of anisotropic hardening behavior for the fracture prediction in high strength steel line pipes. Eng. Fract. Mech. 148, 363–382.

Jafari, M., Bayati Chaleshtari, M.H., 2017. Using dragonfly algorithm for optimization of orthotropic infinite plates with a quasi-triangular cut-out. Eur. J. Mech. A/Solids 66, 1–14.

Javaheri, V., Pohjonen, A., Asperheim, J.I., Ivanov, D., Porter, D., 2019. Physically based modeling, characterization and design of an induction hardening process for a new slurry pipeline steel. Mater. Des. 182, 108047. https://doi.org/10.1016/j.matdes.2019.108047.

Latchoumi, T.P., Ezhilarasi, T.P., Balamurugan, K., 2019. Bio-inspired weighed quantum particle swarm optimization and smooth support vector machine ensembles for identification of abnormalities in medical data. SN Appl. Sci. 1 (10), 1–10.

Loganathan, J., Janakiraman, S., Latchoumi, T.P., 2017. A novel architecture for next generation cellular network using opportunistic spectrum access scheme. J. Adv. Res. Dynam. Control Syst. 12, 1388–1400.

Masadeh, R., A., B., Sharieh, A., 2019. Sea lion optimization algorithm. Sea 10 (5).

Monnet, G., Mai, C., 2019. Prediction of irradiation hardening in austenitic stainless steels: Analytical and crystal plasticity studies. J. Nucl. Mater. 518, 316–325.

Monnet, G., Vincent, L., Gélébart, L., 2019. Multiscale modeling of crystal plasticity in Reactor Pressure Vessel steels: Prediction of irradiation hardening. J. Nucl. Mater. 514, 128–138.

Nath, A., Ray, K.K., Barai, S.V., 2019. Evaluation of ratcheting behaviour in cyclically stable steels through use of a combined kinematic-isotropic hardening rule and a genetic algorithm optimization technique. Int. J. Mech. Sci. 152, 138–150.

Oh, S., Ki, H., 2017. Prediction of hardness and deformation using a 3-D thermal analysis in laser hardening of AISI H13 tool steel. Appl. Therm. Eng. 121, 951–962.

Oh, S., Ki, H., 2019. Deep learning model for predicting hardness distribution in laser heat treatment of AISI H13 tool steel. Appl. Therm. Eng. 153, 583–595.

Özel, T., Nadgir, A., 2002. Prediction of flank wear by using back propagation neural network modeling when cutting hardened H-13 steel with chamfered and honed CBN tools. Int. J. Mach. Tools Manuf 42 (2), 287–297.

Ranjeeth, S., Latchoumi, T.P., Victer Paul, P., 2019. Optimal stochastic gradient descent with multilayer perceptron based student's academic performance prediction model. Recent Adv. Comput. Sci. Commun. https://doi.org/10.2174/2666255813666191116150319.

Ranjeeth, S., Latchoumi, T.P., Paul, P.V., 2020. Role of gender on academic performance based on different parameters: data from secondary school education. Data Brief 29, 105257. https://doi.org/10.1016/j.dib.2020.105257.

Razavi, S.A., Ashrafizadeh, F., Fooladi, S., 2016. Prediction of age hardening parameters for 17–4PH stainless steel by artificial neural network and genetic algorithm. Mater. Sci. Eng. A 675, 147–152.

Schönbauer, B.M., Yanase, K., Endo, M., 2016. VHCF properties and fatigue limit prediction of precipitation hardened 17–4PH stainless steel. Int. J. Fatigue 88, 205–216.

Shamsaei, N., Fatemi, A., 2009. Deformation and fatigue behaviors of case-hardened steels in torsion: experiments and predictions. Int. J. Fatig. 31 (8-9), 1386–1396.

Song, S.-H., Choi, B.-H., 2003. Fatigue characteristics and fatigue limit prediction of an induction case hardened Cr–Mo steel alloy. Mater. Sci. Eng. A 361 (1-2), 15–22.

Sorsa, A., Leiviskä, K., Santa-aho, S., Lepistö, T., 2012. Quantitative prediction of residual stress and hardness in case-hardened steel based on the Barkhausen noise measurement. NDT & E Int. 46, 100–106.

Srinivas, S., Sarvadevabhatla, R.K., Mopuri, K.R., Prabhu, N., Kruthiventi, S.S., Babu, R. V., 2016. A taxonomy of deep convolutional neural nets for computer vision. Front. Robot. AI 2, 36.

Tani, G., Orazi, L., Fortunato, A., 2008. Prediction of hypo eutectoid steel softening due to tempering phenomena in laser surface hardening. CIRP Ann. 57 (1), 209–212.

Torabi, A.R., Kamyab, M., 2019. Mixed mode I/II failure prediction of thin U-notched ductile steel plates with significant strain-hardening and large strain-to-failure: the Fictitious Material Concept. Eur. J. Mech. A/Solids 75, 225–236.

Wang, J.-S., Mulholland, M.D., Olson, G.B., Seidman, D.N., 2013. Prediction of the yield strength of a secondary-hardening steel. Acta Mater. 61 (13), 4939–4952.

Yin, F., Fatemi, A., Bonnen, J., 2010. Variable amplitude fatigue behavior and life predictions of case-hardened steels. Int. J. Fatigue 32 (7), 1126–1135.